JOURNAL OF PHYSICAL ORGANIC CHEMISTRY
J. Phys. Org. Chem. 2002; **15:** 469–475
Published online in Wiley InterScience (www.interscience.wiley.com). DOI: 10.1002/poc.501

Review Commentary

Microsolvated ion stereochemistry[†]

Maurizio Speranza*

Dipartimento di Studi di Chimica e Tecnologia delle Sostanze Biologicamente Attive Università degli Studi di Roma 'La Sapienza,' P.le A. Moro 5, 00185 Rome, Italy

Received 2 September 2001; revised 4 January 2002; accepted 10 January 2002

ABSTRACT: Modeling the evolution of ion–dipole pairs in a dynamic environment, such as in a solvent cage, requires the knowledge of the intrinsic structural and electronic factors governing their behavior in the unsolvated or microsolvated state. An experimental methodology has been developed to this purpose which is based on the generation of tailor-made ionic adducts in gaseous inert media and the investigation of their evolution to products. A survey of the most recent applications of this approach to the gas-phase study of the mechanism and the stereochemistry of ionic substitution and addition reactions is reported. Copyright © 2002 John Wiley & Sons, Ltd.

KEYWORDS: chirality; gas-phase stereochemistry; microsolvated ions; radiolysis; troposelectivity

INTRODUCTION

A 'microsolvated' ion consists of an ion interacting electrostatically with a single neutral molecule. It represents the simplest model for ions generated in a dynamic environment, such as in a solvent cage in solution. The main difference is that the behavior of a 'microsolvated' ion is not perturbed by those environmental factors (solvation, ion pairing, etc.) which normally affect the fate of intimate ion–dipole pairs in solution. Hence a detailed study of the dynamics and the reactivity of microsolvated ions may provide valuable information on the intrinsic factors governing the reaction and how these factors may be influenced by the solvent cage in solution.[1–4]

The evolution of an ion–neutral complex may be accompanied by the rearrangement of its components or simply by their mutual re-orientation before reaction or dissociation. Thus, the knowledge of the structure, the configuration and the initial orientation of the components of the microsolvated system is essential for understanding its reaction stereochemistry.

This paper reports on the stereochemistry of representative addition and substitution reactions taking place within gaseous complexes $[AH{\cdot}B]^+$, wherein AH is the formally charged moiety and B is a nucleophilic molecule. The microsolvated systems investigated contain (i) protonated (*R*)-(−)-2-chlorobutane and an arene,[5] (ii) prochiral α-methylbenzyl cation and methanol;[6] (iii) an *O*-protonated (*R*)-(+)-1-arylethanol and [^{18}O]methanol;[7] and (iv) a tertiary 2-adamantyl cation and [^{18}O]-methanol.[8]

EXPERIMENTAL AND RESULTS

Methodology

Complexes $[AH{\cdot}B]^+$ are generated in an inert gaseous medium at pressures high enough (700–750 Torr; 1 Torr = 133.3 Pa) to allow their complete thermal equilibration. A tailor-made procedure has been used which ensures that the reaction products arise exclusively from the intracomplex reorganization of $[AH{\cdot}B]^+$. Thus, adducts $[AH{\cdot}B]^+$ arise from the intracomplex proton transfer within the $[A{\cdot}HB]^+$ adduct obtained by co-ordination of molecule A around ion BH^+ (path *i* in Scheme 1). The BH^+ precursor is prepared by a route

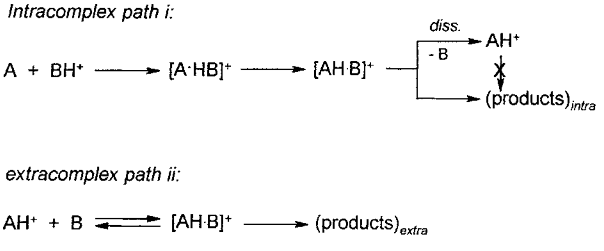

Scheme 1

**Correspondence to:* M. Speranza, Dipartimento di Studi di Chimica e Tecnologia delle Sostanze Biologicamente Attive, Università degli Studi di Roma 'La Sapienza,' P.le A. Moro 5, 00185 Rome, Italy.
E-mail: maurizio.speranza@uniromal.it

[†] Presented at the 8th European Symposium on Organic Reactivity (ESOR-8), Cavtat (Dubrovnik), Croatia, September 2001.

Contract/grant sponsor: Ministero della Università e della Ricerca Scientifica e Tecnologica (MURST).
Contract/grant sponsor: Consiglio Nazionale delle Ricerche (CNR).

Copyright © 2002 John Wiley & Sons, Ltd.

excluding the presence of its conjugate base. For instance, the $[AH{\cdot}B]^+$ complex with AH^+ = tertiary 2-adamantyl cation and $B = CH_3{}^{18}OH$ is generated by intracomplex proton transfer within the adduct between 2-methylene-5-X-adamantane (A) with $CH_3{}^{18}OH_2^+$ (BH^+). Ions $CH_3{}^{18}OH_2^+$ are in turn formed in the gas phase by methylation of $H_2{}^{18}O$ with the $(CH_3)_2F^+$ ions obtained in known yields by γ-radiolysis of CH_3F. In this way, ions $CH_3{}^{18}OH_2^+$ are generated in complete absence of their conjugate $CH_3{}^{18}OH$ base and, hence, their reaction products, i.e. the ^{18}O-labeled 2-methyl-2-methoxy-5-X-adamantanes, are bound to arise exclusively from the intracomplex addition of the incipient 2-adamantyl cation to the putative $CH_3{}^{18}OH$ molecule.

In some instances, the outcome of the intracomplex process *i* in Scheme 1 is confronted with that of the direct reaction between unsolvated AH^+ ion (or its rearranged form) and an external B molecule (the ‘extracomplex’ path *ii* in Scheme 1). Taking again the above example, AH^+ = tertiary 2-adamantyl cation is simply obtained by protonation of 2-methylene-5-X-adamantane with $C_nH_5^+$ ($n = 1, 2$) ions, formed by γ-radiolysis of gaseous CH_4. The ‘extracomplex’ path *ii* in Scheme 1 takes place by coordination of the so-formed 2-adamantyl cation with external $CH_3{}^{18}OH$ molecules, present as a massive additive in the irradiated mixture.

Arenium ion–(*R*)-(−)-2-chlorobutane adducts

A crucial question concerns the chemical identity and the relative spatial arrangement of the components of a microsolvated system, two features of paramount importance to assess the kinetic and the mechanistic role of the corresponding ion–dipole pairs in solution. In the example, reported in this section, Aschi *et al.* considered the ion–molecule complexes involved in the classical Friedel–Crafts alkylation of arenes.[5]

At 300 K and under Fourier transform ion cyclotron resonance (FT-ICR) conditions, the benzenium ion $C_6H_7^+$ reacts with 2-chlorobutane C_4H_9Cl to give the $C_{10}H_{15}^+$ ion with a rate constant of 5×10^{-11} cm^3 molecule^{-1} s^{-1}, corresponding to a collision efficiency of 2.5% [Eqns (1a) and (1b)].[9]

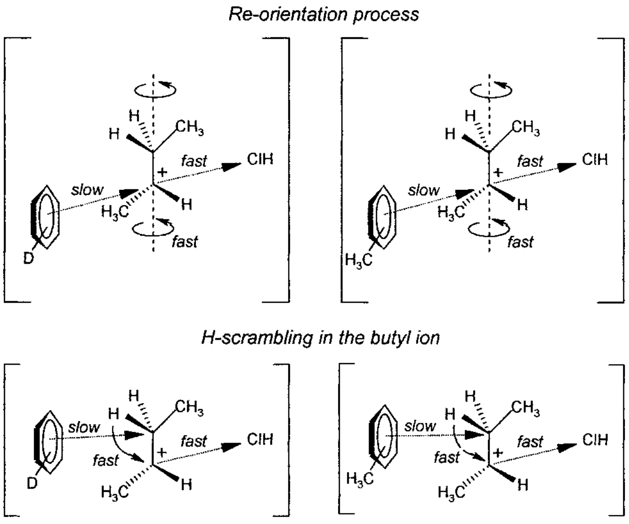

Chart 1

No information is available from this experiment as to the detailed path of formation of $C_{10}H_{15}^+$, whether via Eqn. (1a) or Eqn. (1b). Further, no information is available as to the spatial relationship and the dynamics of the species present in the second complex of Eqns (1). To answer these questions, the $^{12}C_6H_6D^+$ arenium ion was prepared in the gas phase by deuteronation of $^{12}C_6H_6$ with radiolytic $C_nD_5^+$ ($n = 1, 2$) ions. Similarly, the $^{12}C_6H_6CH_3^+$ arenium ion was generated in the gas phase by methylation of $^{12}C_6H_6$ with radiolytic $(CH_3)_2F^+$. Either arenium ions were allowed to react at 700–750 Torr with (*R*)-(−)-2-chlorobutane.[5] The corresponding 2-arylbutanes, recovered among the radiolytic products, display complete racemization which points to their formation as proceeding exclusively via Eqn. (1b). This implies that alkylation follows an S_N1 mechanism, i.e. a process wherein covalent bond breaking precedes covalent bond formation as in the three body adduct of Eqn. (1b), whose individual components are not constrained in a fixed geometry, but are free to reorientate or to rearrange before addition (Chart 1).

Chiral α-methylbenzyl cation–methanol adducts

The rate of ^{18}O exchange between water and the chiral labeled alcohols as a function of racemization has been extensively used as a criterion for discriminating the S_N2 from the S_N1 solvolytic mechanisms in solution. The expected ratio of exchange vs racemization rate is 0.5 for the S_N2 mechanism and 1.0 for a pure S_N1 process.[10] With chiral ^{18}O-enriched 1-phenylethanol in aqueous

$$C_6H_7^+ + C_4H_9Cl \rightarrow \left[C_6H_7^+{\cdot}C_4H_9Cl\right] \rightarrow \left[C_6H_6{\cdot}C_4H_9ClH^+\right] \rightarrow C_{10}H_{15}^+ + HCl \qquad (1a)$$

$$C_6H_7^+ + C_4H_9Cl \rightarrow \left[C_6H_7^+{\cdot}C_4H_9Cl\right] \rightarrow \left[C_6H_6{\cdot}C_4H_9^+{\cdot}HCl\right] \rightarrow C_{10}H_{15}^+ + HCl \qquad (1b)$$

Copyright © 2002 John Wiley & Sons, Ltd.

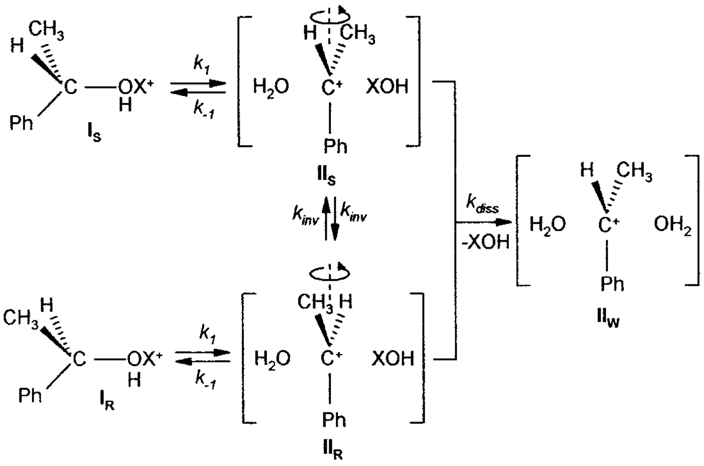

Scheme 2

acids, this ratio is found to be 0.84 ± 0.05. This value has been interpreted in terms of the kinetic pattern of Scheme 2 involving the reversible dissociation of the oxonium ion $\mathbf{I_S}$ (XOH = $H_2{}^{18}O$) to the chiral intimate ion–dipole pair $\mathbf{II_S}$ ($k_{-1} > k_{inv}$). In $\mathbf{II_S}$, the leaving $H_2{}^{18}O$ molecule does not equilibrate immediately with the solvent (i.e. $H_2{}^{16}O$), but remains closely associated with the ion. This means that k_{inv} is of the same order of magnitude of k_{diss}.[11,12] In contrast, the rate constant ratio of exchange vs racemization of chiral 1-phenyl-1-methoxyethane in acidic acetonitrile–water solutions is as large as 0.99. The closeness of this value to that of a pure S_N1 mechanism indicates that, in Scheme 2 (XOH = CH_3OH), either k_{inv} is many orders of magnitude lower than k_{diss} or, if not, that internal return is negligible ($k_{-1} \ll k_{inv}$).[13] This kinetic ambiguity prevents identification of the actual factors hindering inversion in $\mathbf{II_S}$ (XOH = CH_3OH).

Removal of this ambiguity was due to Filippi *et al.*,[6] who prepared the chiral oxonium ion $\mathbf{I_S}$ (XOH = CH_3OH) in the gas phase by methylation of *S*-(−)-1-phenylethanol ($\mathbf{1_S}$) with $(CH_3)_2Cl^+$ ions (Scheme 3). The latter ions are generated by γ-radiolysis of CH_3Cl, present as bulk component (720 Torr; 25–160 °C) of gaseous mixtures containing traces of the alcoholic substrate, of $H_2{}^{18}O$, of a radical scavenger (i.e. O_2), and of a powerful base [i.e. $(C_2H_5)_3N$].

Detailed information on the reorganization dynamics of the intimate ion–dipole pair $\mathbf{II_S}$, arising from $\mathbf{I_S}$ by C—O bond dissociation, is inferred from the kinetic study of the intracomplex inversion of configuration of $\mathbf{I_S}$ vs its dissociation to α-methylbenzyl cation (**III**) and CH_3OH. The results point to k_{inv} values that are anything but negligible relative to k_{diss} rate constants within the entire temperature range investigated (25–160 °C). Indeed, k_{inv} are just 2–4 times lower than k_{diss}. This implies that, in acidic media, the hindered inversion of $\mathbf{I_S}$ (XOH = CH_3OH) has to be ascribed to the lack of appreciable $\mathbf{II_S} \rightarrow \mathbf{I_S}$ (and $\mathbf{II_R} \rightarrow \mathbf{I_R}$) internal return ($k_{-1} \ll k_{inv}$; Scheme 2), rather than to k_{inv} negligible relative to k_{diss}.[13] Accordingly, the difference in the behavior of $\mathbf{II_S}$ (and

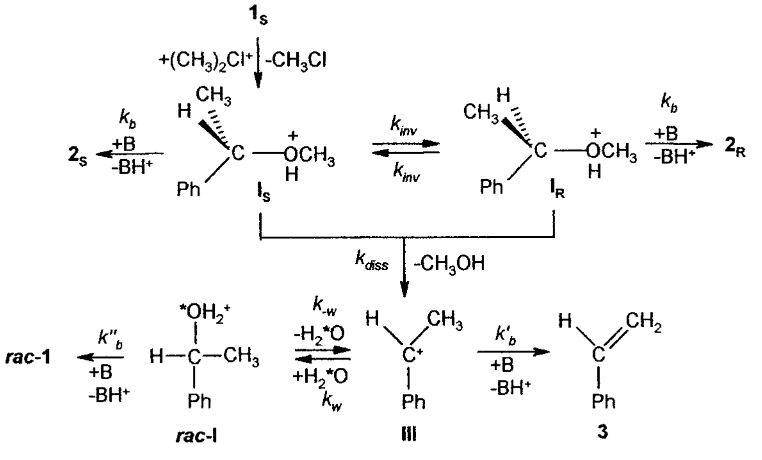

Scheme 3

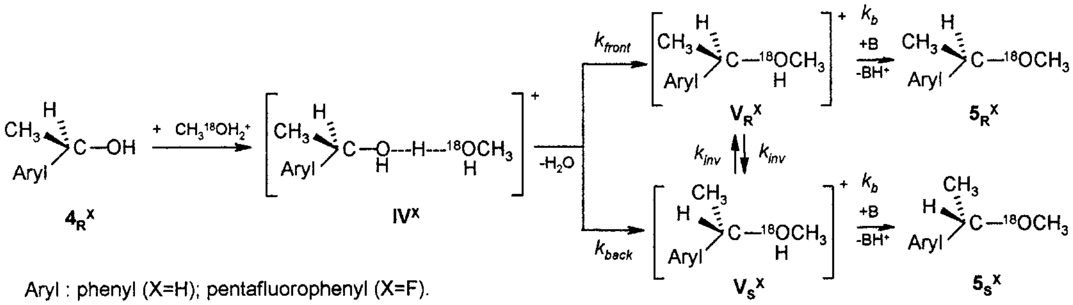

Aryl : phenyl (X=H); pentafluorophenyl (X=F).

Scheme 4

$\mathbf{II_R}$) in acidic solution essentially reduces to $k_{-1} > k_{\text{diss}}$, when XOH = $H_2{}^{18}O$, and $k_{-1} \ll k_{\text{diss}}$, when XOH = CH_3OH.

Quantum chemical calculations at the B3LYP/6–31G* level of theory were employed to gain some insight into the reasons for this dual behavior. Despite the intrinsic limitations of the B3LYP functional in describing non-covalent interactions and the necessarily limited dimensions of the 6–31G* basis set employed, nevertheless, calculations qualitatively indicate that the $\mathbf{I_S} \rightleftharpoons \mathbf{I_R}$ (XOH = CH_3OH) transition structures are placed late along the reaction coordinate. The CH_3OH moiety is enough removed from the benzyl ion moiety to start interacting with the solvent cage. These interactions favor $\mathbf{II_S} \rightarrow \mathbf{II_W}$ dissociation and prevent efficient $\mathbf{II_S} \rightarrow \mathbf{I_S}$ internal return ($k_{-1} < k_{\text{diss}}$ in Scheme 2).[13] The $\mathbf{I_S} \rightleftharpoons \mathbf{I_R}$ (XOH = $H_2{}^{18}O$) transition structures are instead placed much earlier along the reaction coordinate so as to resemble the starting $\mathbf{I_S}$ ion. In them, the moving $H_2{}^{18}O$, less basic than CH_3OH, sits nearby the departure face of the still flexible benzylic residue and does not appreciably interact with its acidic hydrogens. A surplus of energy is needed to remove the $H_2{}^{18}O$ moiety far enough to establish appreciable interactions with the solvent cage and to promote $\mathbf{II_S} \rightarrow \mathbf{II_W}$ dissociation. As a consequence, $\mathbf{II_S} \rightarrow \mathbf{I_S}$ internal return can efficiently compete with $H_2{}^{18}O$ diffusion to the aqueous cage ($k_{-1} > k_{\text{diss}}$). Besides, the shielding effect of the $H_2{}^{18}O$ leaving group accounts for the observed prevalence of the inversion of configuration in the H_2O-to-$H_2{}^{18}O$ exchange in solution.[11,12]

(*R*)-(+)-1-Arylethanol–$CH_3{}^{18}OH_2^+$ adducts

It is well established that bimolecular S_N2 reactions generally involve predominant inversion of configuration of the reaction center. Unimolecular S_N1 displacements instead proceed through the intermediacy of free carbocations and, therefore, usually lead to racemates. However, many alleged S_N1 solvolyses do not give fully racemized products. The enantiomer in excess often, but not always, corresponds to inversion. Furthermore, the stereochemical distribution of products may be highly sensitive to the solvolytic conditions.[14] These observations have led to the concept of competing[15–17] or mixed[17–19] S_N1–S_N2 mechanisms. More recently, the existence itself of S_N1 reactions has been put into question.[20]

Some obscure facets of this intricate picture were unveiled by Filippi and Speranza, who investigated the stereochemistry and the intimate mechanism of a model 'solvolytic' reaction taking place in an ion–dipole pair in the gaseous phase.[7] Adduct $\mathbf{IV^X}$ is obtained in the gas phase by association of the relevant chiral alcohol $\mathbf{4_R{}^X}$ with the $CH_3{}^{18}OH_2^+$ ion, generated by γ-radiolysis of CH_3F–$H_2{}^{18}O$ mixtures (Scheme 4). As mentioned above, the absence of neutral nucleophile molecules, i.e. $CH_3{}^{18}OH$, in the reaction medium ensures that the ^{18}O-labeled ethers $\mathbf{5_R{}^X}$ and $\mathbf{5_S{}^X}$ in Scheme 4 arise exclusively from the intracomplex 'solvolysis' of $\mathbf{IV^X}$.

Ancillary experiments have been carried out to evaluate the extent of $\mathbf{V_R{}^X} \rightleftharpoons \mathbf{V_S{}^X}$ interconversion (k_{inv} in Scheme 4) prior to neutralization (k_b in Scheme 4). The gaseous samples used for this purpose contained CH_3Cl, instead of CH_3F, as the bulk component. This prevents the radiolytic formation of $CH_3{}^{18}OH_2^+$ ions to any significant extent. In fact, unlike $(CH_3)_2F^+$, $(CH_3)_2Cl^+$ ions are essentially inert towards the water molecules present in the mixture.[21] As a consequence, the oxonium intermediates $\mathbf{V_R{}^X}$ are directly formed from $(CH_3)_2Cl^+$ methylation of $\mathbf{4_R{}^X}$, and any contribution from other conceivable pathways, including the second step in Scheme 4, can be safely excluded.

The experimental results point to intracomplex 'solvolysis' in $\mathbf{IV^X}$ as proceeding through the intermediacy of the relevant benzyl cation (a pure S_N1 mechanism). 'Solvolysis' of $\mathbf{IV^H}$ leads to complete racemization at $T > 50\,°C$, whereas at $T < 50\,°C$ the reaction displays a preferential retention of configuration. Predominant retention of configuration is also observed in the intracomplex 'solvolysis' of $\mathbf{IV^F}$. The exothermic intracomplex displacement in $\mathbf{IV^H}$ proceeds through TSs characterized by non-covalent interactions between the stable benzyl cation and the nucleophile–leaving group pair (an S_N1 process). The formation of the $\mathbf{V_R{}^H}$–

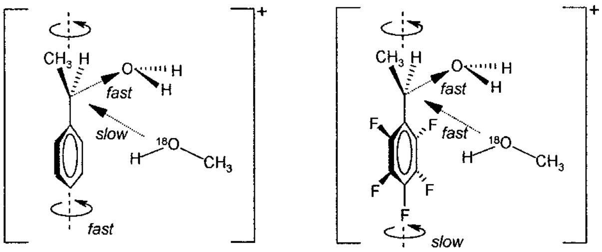

$\mathbf{VI^H}$ $\mathbf{VI^F}$

Chart 2

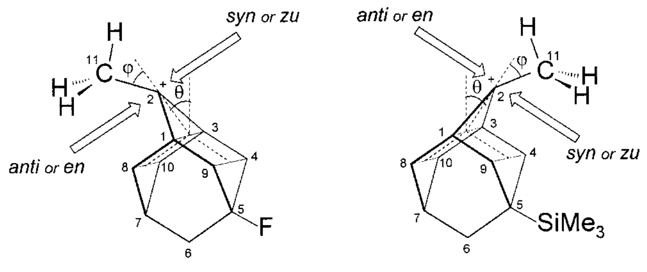

(VII$_F$) (VII$_{Si}$)

Chart 3

$\mathbf{V_S^H}$ racemate from $\mathbf{IV^H}$ at $T > 50\,°C$ is entirely consistent with this view. In this frame, the slight predominance of retained $\mathbf{V_R^H}$ over the inverted $\mathbf{V_S^H}$, observed at $T < 50\,°C$, is accounted for by a free rotation of the benzylic moiety of complex $\mathbf{VI^H}$ (Chart 2) slower than its bonding to $CH_3{}^{18}OH$. In fact, the procedure adopted to generate $\mathbf{IV^H}$ in the gas phase requires that the $CH_3{}^{18}OH$ moiety resides initially in the same region of space containing the leaving group (complex $\mathbf{VI^H}$ in Chart 2). In the absence of any intracomplex rotation of the benzylic moiety of $\mathbf{VI^H}$, $CH_3{}^{18}OH$ is spatially situated to attack from the frontside (a *troposelective* reaction). At higher temperatures, this positional advantage is annulled and the $\mathbf{V_R^H}$–$\mathbf{V_S^H}$ racemate is formed.

The intracomplex 'solvolysis' of $\mathbf{IV^F}$ can be considered highly troposelective since it involves predominant retention of configuration (88% at 25 °C). Inductive and resonance effects of the ring fluorine substituents reduce appreciably the stabilization energy of the α-methylpentafluorobenzyl cation relative to the unsubstituted homolog. This implies that the interactions between the nucleophile–leaving group and benzylic moiety in complex $\mathbf{VI^F}$ (Chart 2) should be stronger than those operating in adduct $\mathbf{VI^H}$. As a consequence, free rotation of benzylic moiety in $\mathbf{VI^F}$ is slow relative to covalent bonding with $CH_3{}^{18}OH$.

The above gas-phase picture may represent a guideline for understanding the mechanism and the stereochemistry of substitution reactions in the solvent cage. The results of gas-phase $\mathbf{4_R^H}$ 'solvolysis' demonstrate the existence of a pure S_N1 mechanism. Fast rotation of the benzylic moiety in the complex $\mathbf{VI^H}$ ($T > 50\,°C$) explains the formation of the product racemate. If rotation is hampered by significant ion-nucleophile interactions (as in $\mathbf{4^F}$ and $\mathbf{4^H}$ at $T < 50\,°C$), predominant retention of configuration is observed. This may explain why some solvolytic reactions lead to a slight excess of the retained product in the liquid phase. However, the presence of the solvent cage may alter this picture and favor inversion of configuration even if a pure S_N1 solvolysis is taking place. This may happen when reorientation of the ion in the cage is slow and if the presence of the leaving group hampers the approach of the nucleophile from the frontside. However, inversion of configuration predominates even when the relative motionlessness of the ion in the solvent cage is due to a partial covalency of its interactions with the leaving group and the nucleophilic solvent (an S_N2 process). It is concluded that the solvolytic reactions are mostly governed by the lifetime and the dynamics of the species involved and, if occurring in solution, by the nature of the solvent cage. Their rigid subdivision into the S_N1 and S_N2 mechanistic categories appears inadequate and the use of their stereochemistry as a mechanistic probe can be highly misleading.

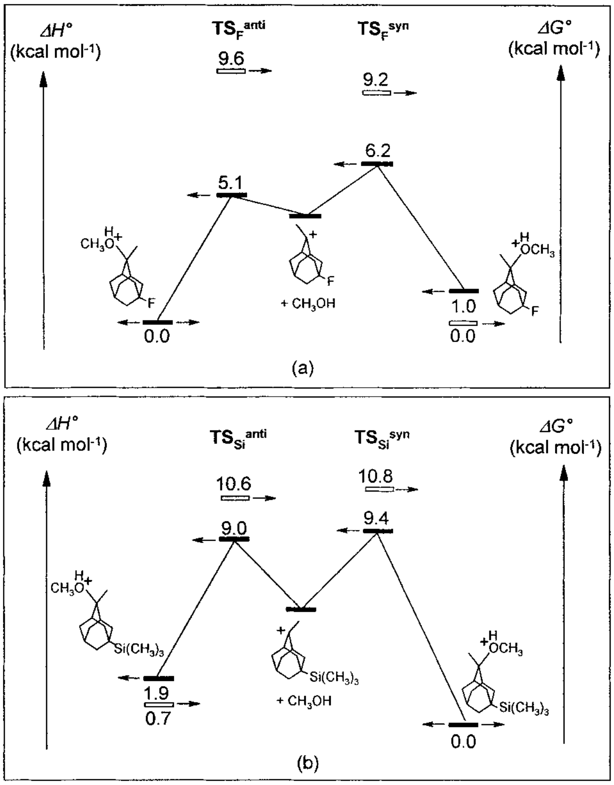

Figure 1. The 298 K enthalpy (solid bars) and free energy (open bars) profiles of the gas-phase extracomplex addition of $CH_3{}^{18}OH$ to 2-methyl-5-fluoro-2-adamantyl (a) and 2-methyl-5-trimethylsilyl-2-adamantyl cations (b) (path *ii* in Scheme 1)

Copyright © 2002 John Wiley & Sons, Ltd.

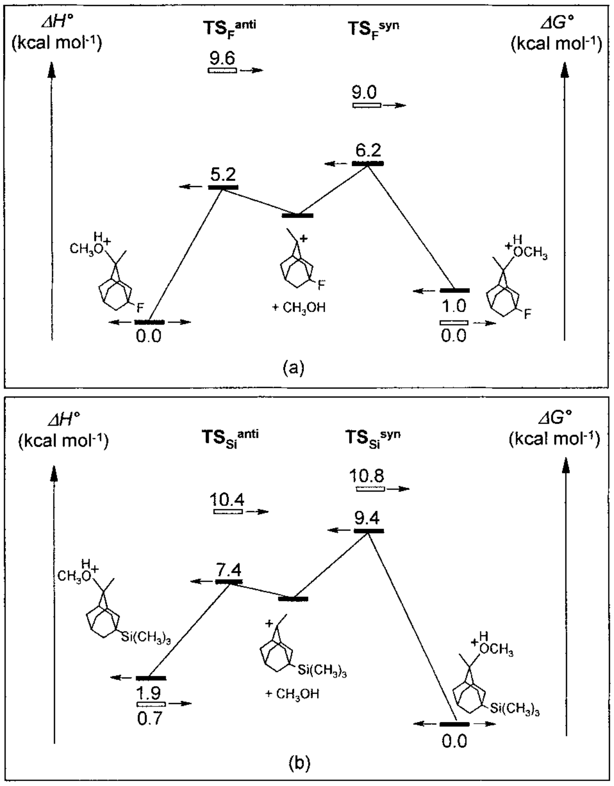

Figure 2. The 298 K enthalpy (solid bars) and free energy (open bars) profiles of the gas-phase intracomplex addition of $CH_3{}^{18}OH$ to 2-methyl-5-fluoro-2-adamantyl (a) and 2-methyl-5-trimethylsilyl-2-adamantyl cations (b) (path *i* in Scheme 1)

2-Methylene-5-X-adamantane–$CH_3{}^{18}OH_2^+$ adducts

The intrinsic factors governing the diastereofacial selectivity in the intra- and extracomplex addition of 2-methyl-5-X-2-adamantyl cations [X = F (**VII**$_F$), $Si(CH_3)_3$ (**VII**$_{Si}$)] with methanol have been the object of a comprehensive gas-phase study carried out by Filippi *et al.* ($P = 750$ Torr; $T = 20$–80 °C; Chart 3).[8] At all temperatures, a preferred *syn* selectivity is observed with **VII**$_F$, whereas **VII**$_{Si}$ exhibits a preferential *anti* selectivity.

The experimental evidence is summarized in Figs 1 and 2. Accordingly; (1) *anti* attack of CH_3OH on both ions **VII**$_F$ and **VII**$_{Si}$ is enthalpically favored over the competing *syn* addition irrespective of whether it proceeds through the intracomplex (*ii* in Scheme 1) or the extracomplex pathway (*ii* in Scheme 1); (2) the preferred *syn* diastereoselectivity, observed with ion **VII**$_F$ at $T \geq 20$ °C, is determined by large adverse *entropic* factors which overwhelm the enthalpy terms [Figs 1(a) and 2(a)]; (3) contrariwise, the *anti* > *syn* selectivity, measured with ion **VII**$_{Si}$ at $T \geq 20$ °C, is essentially governed by the relevant activation enthalpies since adverse entropy factors plays a minor role [Figs 1(b) and 2(b)]; (4) entropy factors are more important in the intracomplex *anti* attack of CH_3OH on **VII**$_{Si}$ [Fig. 2(b)] than in the extracomplex one [Fig. 1(b)].

Kinetic and thermochemical considerations point to the gas-phase addition of methanol to **VII**$_F$ as proceeding through tight transition structures (**TS**$_F^{syn}$ and **TS**$_F^{anti}$), whereas the same reaction on **VII**$_{Si}$ involves much looser transition structures (**TS**$_{Si}^{syn}$ and **TS**$_{Si}^{anti}$). Comparison of Figs 1(b) and 2(b) shows that, while the extra- (*ii* in Chart 1) and the intracomplex *syn* addition (*i* in Chart 1) in **VII**$_{Si}$ exhibit equally large activation barriers, the enthalpy barrier involved in the intracomplex *anti* addition in **VII**$_{Si}$ [Fig. 2(b)] is 1.6 kcal mol^{-1} lower than that governing the corresponding extracomplex reaction [Fig. 1(b)]. This suggests that, while the *syn* addition in **VII**$_{Si}$ proceeds through a single loose transition structure **TS**$_{Si}^{syn}$, the corresponding *anti* addition in **VII**$_{Si}$ may involve two different **TS**$_{Si}^{anti}$ transition structures with very similar activation free energies in the temperature range investigated. One is characterized by a loose structure similar to that involved in the competing *syn* addition [Fig. 1(b)]. The lower enthalpy value associated with **TS**$_{Si}^{anti}$ in Fig. 2(b) is instead consistent with a much tighter structure. The fact that the latter **TS**$_{Si}^{anti}$ is involved in the intracomplex addition, where the putative $CH_3{}^{18}OH$ nucleophile is necessarily proton bonded to the CH_3 hydrogens of the incipient ion **VII**$_{Si}$, provides strong support in favor of a structure where the methanol molecule is specifically coordinated between the C2 center and the adjacent acidic CH_3 hydrogens of the **VII**$_{Si}$ moiety.

In their seminal work, le Noble and co-workers[22–24] reported on the diastereoselectivity of chloride ion attack on 2-methyl-5-fluoro-2-adamantyl cations, generated in CH_2Cl_2 by reaction of gaseous HCl with (*E*)- and (*Z*)-2-methyl-5-fluoro-2-hydroxyadamantane. The dominant product from this reaction is the (*Z*)-chloride which exceeds the (*E*)-chloride by a factor of 3:1 or more. le Noble *et al.* explained the origin of this stereoselectivity in terms of the differential hyperconjugative stabilization of two rapidly equilibrating σ-delocalized 2-methyl-5-fluoro-2-adamantyl cations.

This picture is not corroborated by the B3LYP/6–31G* calculations, pointing to a single *syn*-pyramidalized structure for X = F and a single *anti*-pyramidalized structure for $X = SiMe_3$ (Chart 3). The kinetic results demonstrated that the gas-phase diastereoselectivity of 2-methyl-5-X-2-adamantyl cations towards methanol is mainly determined by the relative stability of their reaction products and that entropic factors may play a major role. Further, it should be noted that gas-phase selectivity is less pronounced than that measured by Adcock and co-workers in solution towards the chloride anion.[25,26] This difference cannot be satisfactory explained in terms of equilibrating *syn/anti* structures, allowed by specific solvent effects in solution. In fact, their conceivable coexistence in solution would lead to a

Copyright © 2002 John Wiley & Sons, Ltd.

diastereoselectivity lower and not greater than that measured in the gas phase. Hence the higher diastereoselectivity monitored in solution may find a plausible rationale only in the differential solvation of the two faces of a pyramidalized 2-methyl-5-substituted-2-adamantyl cation. Indeed, differential solvation may modify the cage viscosity contribution to the addition activation barrier as well as the associated activation entropy. This may account for the pronounced substituent and solvent effects on the diastereoselectivity of 2-methyl-5-X-2-adamantyl cations observed in solution.

CONCLUSIONS

The advantages connected with studying the stereochemistry of microsolvated systems in the gas phase instead of in a solvent cage come from the possibility of making precise statements about the factors governing their dynamics and kinetics in the lack of any perturbing environmental effects (solvation, ion pairing, cage viscosity, etc.). These effects may be evaluated by comparing the behavior of a microsolvated systems with that of the corresponding system in solution. An experimental methodology has been developed for this purpose, the results of which demonstrate that ionic processes in solution are mostly governed by the lifetime and the dynamics of intimate ion–neutral complexes and that these can in turn be profoundly influenced by the nature of the solvent cage and its uneven arrangement around the charged intermediate.

Acknowledgements

This work was supported by the Ministero della Università e della Ricerca Scientifica e Tecnologica (MURST) and the Consiglio Nazionale delle Ricerche (CNR).

REFERENCES

1. Morton TH. *Tetrahedron* 1982; **38**: 3195–3243.
2. Bowen RD. *Acc. Chem. Res.* 1991; **24**: 364–371.
3. Morton TH. *Org. Mass Spectrom.* 1992; **27**: 353–368.
4. McAdoo DJ, Morton TH. *Acc. Chem. Res.* 1993; **26**: 295–302.
5. Aschi M, Cacace F, Troiani A. *Angew. Chem., Int. Ed. Engl.* 1997; **36**: 83–85.
6. Filippi A, Gasparrini F, Speranza M. *J. Am. Chem. Soc.* 2001; **123**: 2251–2254.
7. Filippi A, Speranza M. *J. Am. Chem. Soc.* 2001; **123**: 6077–6082.
8. Filippi A, Trout NA, Brunelle P, Adcock W, Sorensen TS, Speranza M. *J. Am. Chem. Soc.* 2001; **123**: 6396–6403.
9. Aschi M, Attinà M, Cacace F. *Res. Chem. Intermed.* 1996; **22**: 645–658.
10. For a review, see: Samuel D, Silver B. *Adv. Phys. Org. Chem.* 1965; **3**: 128–186.
11. Merritt MV, Bell SJ, Cheon HJ, Darlington JA, Dugger TL, Elliott NB, Fairbrother GL, Melendez CS, Smith EV, Schwartz PL. *J. Am. Chem. Soc.* 1990; **112**: 3560–3566, and references cited therein.
12. Merritt MV, Anderson DB, Basu KA, Chang IW, Cheon HJ, Mukundan NE, Flannery CA, Kim AY, Vaishampayan A, Yens DA. *J. Am. Chem. Soc.* 1994; **116**: 5551–5559, and references cited therein.
13. Thibblin A. *J. Phys. Org. Chem.* 1993; **6**: 287–292, and references cited therein.
14. March J. *Advanced Organic Chemistry*. Wiley: New York, 1985; 357–362.
15. Dostrovsky I, Hughes ED, Ingold CK. *J. Chem. Soc.* 1946; 173–177.
16. Bentley TW, Bowen CT, Parker W, Watt CIF. *J. Am. Chem. Soc.* 1979; **101**: 2486–2488.
17. Jencks WP. *Chem. Soc. Rev.* 1982; **10**: 345–375.
18. Bentley TW, Bowen CT, Morten DH, Schleyer PvR. *J. Am. Chem. Soc.* 1981; **103**: 5466–5475.
19. Bentley TW, Bowen CT. *J. Chem. Soc., Perkin Trans. 2* 1978; 557–562.
20. Dale J. *J. Chem. Educ.* 1998; **75**: 1482–1485.
21. Speranza M, Troiani A. *J. Org. Chem.* 1998; **63**: 1020–1026.
22. Cheung CK, Tseng LT, Lin MH, Srivastava S, le Noble WJ. *J. Am. Chem. Soc.* 1986; **108**: 1598–1605.
23. Schulman EM, Cheung CK, Merbach AE, Yamada H, le Noble WJ. *J. Am. Chem. Soc.* 1987; **109**: 7206–7207.
24. Srivastava S, le Noble WJ. *J. Am. Chem. Soc.* 1987; **109**: 5874–5875.
25. Adcock W, Cotton J, Trout NA. *J. Org. Chem.* 1994; **59**: 1867–1876.
26. Adcock W, Head NJ, Lokan NR, Trout NA. *J. Org. Chem.* 1997; **62**: 6177–6182.

Copyright © 2002 John Wiley & Sons, Ltd.